Optical polarization of localized hole spins in p-doped quantum wells

M. Studer,[1,2] M. Hirmer,[3] D. Schuh,[3] W. Wegscheider,[1] K. Ensslin,[1] and G. Salis*[2]

[1] *Solid State Physics Laboratory, ETH Zurich, 8093 Zurich, Switzerland*
[2] *IBM Research–Zurich, Säumerstrasse 4, 8803 Rüschlikon, Switzerland*
[3] *Institut für Experimentelle und Angewandte Physik, Universität Regensburg, 93040 Regensburg, Germany*

The initialization of spin polarization in localized hole states is investigated using time-resolved Kerr rotation. We find that the sign of the polarization depends on the magnetic field, and the power and the wavelength of the circularly polarized pump pulse. An analysis of the spin dynamics and the spin-initialization process shows that two mechanisms are responsible for spin polarization with opposite sign: The difference of the g factor between the localized holes and the trions, as well as the capturing process of dark excitons by the localized hole states.

PACS numbers:

Localized hole spins in p-doped III-V semiconductors can have considerably long spin lifetimes[1] in the range of 100 μs and coherence times[2] on the order of μs. Holes or electrons can be localized in natural quantum dots (QDs) formed due to potential fluctuations in quantum wells (QWs).[3,4] The spin of localized hole states in p-doped GaAs/AlGaAs QWs has been studied using time-resolved Kerr rotation (TRKR).[5–7] Information on hole spins can also be obtained in n-doped QW structures by studying the recombination of an optically excited hole spin with a resident electron.[8,9] The reliable polarization of hole spins in QDs is one of the key requirements necessary to study this quantum system. Possible polarization mechanisms make use of the properties of the optically excited positively charged trion that are different compared to those of the bare hole, e.g. the different interaction with nuclear spins[10] or the different g factor.[6]

In our study, a p-doped QW is excited with circularly polarized photons giving rise to two competing spin polarization mechanisms leading to polarization of an ensemble of localized holes. The two mechanisms polarize the spins with opposite signs, and their relative strength depends on the external magnetic field ($B_{\rm ext}$), the pump power ($P_{\rm P}$) and the wavelength (λ) of the pump beam. The first mechanism is found to rely on the difference of the trion and the hole g factors and disappears for $B_{\rm ext} = 0$. The second mechanism remains effective for $B_{\rm ext} = 0$ and strongly depends on $P_{\rm P}$ and λ. The relative strength of the two mechanisms can therefore be controlled by the properties of the pump pulse. We show that the second mechanism can be explained by a capturing of dark excitons by the localized holes.

To generate and study the spin polarization, we employ time-resolved Kerr rotation (TRKR). Circularly polarized laser pulses focused onto a spot with a diameter of about 40 μm pump the optical transitions and generate spin-polarized excitons and trions. The generation of a trion with an electron spin up using a σ^--polarized photon is depicted in Fig 1(c). After the decay of these excited states, an ensemble of localized hole spins remains polarized (see discussion below). The polarization of these hole spins is detected using linearly polarized probe pulses that are delayed by a time Δt with respect to the pump pulses. The reflected probe pulses are analyzed and reveal the component of spin polarization along the QW growth direction $\mathbf{z}$ at time Δt by a small rotation $\Theta_{\rm K}$ of the polarization angle. We use a cascaded lock-in technique where both the circular polarization of the pump pulse as well as the probe intensity are modulated. The sample is mounted in a cryostat and cooled to 1.6 K. The external magnetic field is applied at an angle $\beta = 3°$ with respect to the sample plane [see insert of Fig. 1(a)]. We investigate a 4-nm-wide remotely doped GaAs/AlGaAs QW with a hole sheet density of 1.1×10^{15} m^{-2} and a mobility of 1.3 m^2(Vs)$^{-1}$ measured at 1.3 K.

Figure 1(a) shows experimental TRKR signals at three different magnetic fields. At $B_{\rm ext} > 0$, $\Theta_{\rm K}$ is the sum of two exponentially decaying cosine functions and a non-oscillating exponential function. The short-lived oscillation (best seen at $B_{\rm ext} = 4$ T and $0 < \Delta t < 100$ ps) is attributed[5] to the trion spin which is determined by the spin of the electron in the trion and therefore precesses with the electron g factor g_e. We measure a decay time of $\tau_{\rm T}$=80 ps and g_e=0.34. We assume that this part of the signal decays mainly due to the recombination rate of the trions $(1/\tau_R)$[7], i.e. $\tau_{\rm T} \cong \tau_{\rm R}$. The longer-lived part of $\Theta_{\rm K}$ originates from the localized hole spins.[5] Due to the tilt angle β and the strong anisotropy of the hole g factor, the precession axis of the hole spins is tilted out of plane[6] by an angle $\alpha > \beta$ [see insert of Fig. 1(a)]. The Kerr signal is proportional to the projection of the spins of the ensemble along $\mathbf{z}$ and therefore also has a non-oscillating part. Note that for the two curves at $B_{\rm ext} = 0.5$ and 4 T, the trion and both parts of the hole signal have a positive amplitude.

The situation for $B_{\rm ext}$=0 is strikingly different. There, $\Theta_{\rm K}$ can be described by a superposition of two exponentials with amplitudes of opposite sign. While the short-lived trion signal is still positive, the long-lived sig-

*gsa@zurich.ibm.com

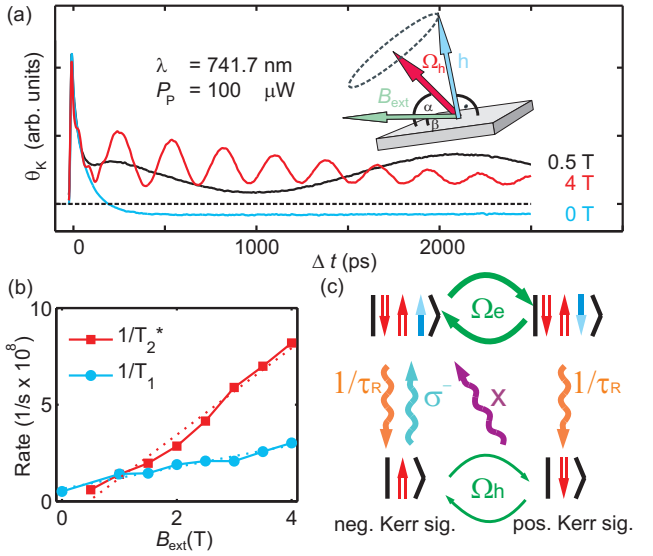

FIG. 1: (Color online) (a) Experimental TRKR signals for three $B_{\rm ext}$ values for a probe power of 20 μW. The insert shows a schematic precession of the hole spins (h) in the tilted $B_{\rm ext}$ around the precession axis Ω_h. (b) Dephasing rates vs. $B_{\rm ext}$. (c) Localized hole and trion states: Arrows symbolize the transitions between the four states.

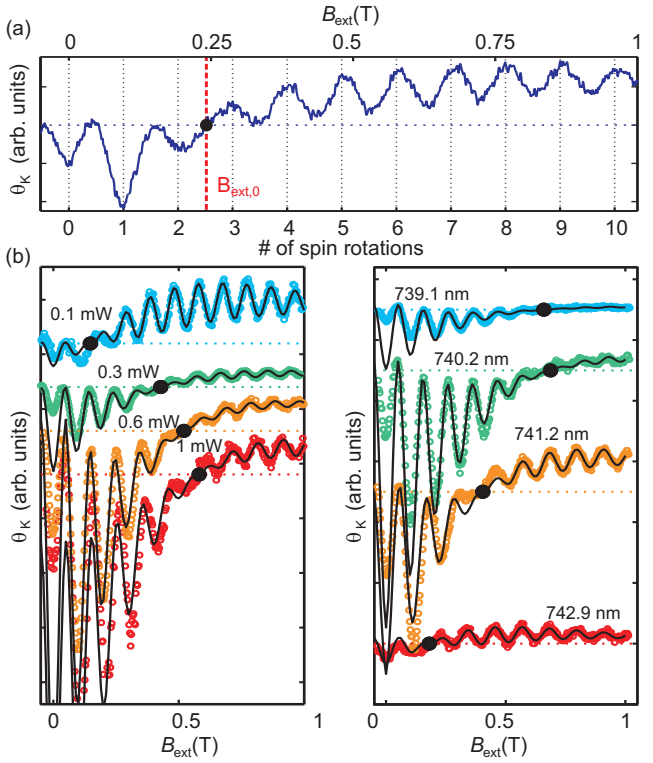

FIG. 2: (Color online) Kerr rotation measurements vs. $B_{\rm ext}$ at Δt = 12.4 ns using a probe power of 10 μW. (a) λ = 741.2 nm and $P_{\rm P}$=0.2 mW. The vertical line and the dot mark the $B_{\rm ext}$ value where $I_{\rm h}$ = 0. (b) left panel: λ = 741.2 nm and varying $P_{\rm P}$. Right panel: $P_{\rm P}$ = 500 μW and varying λ. For all measurements in (b) the fits are superimposed as solid lines.

nal from the localized holes now has a negative amplitude. From this, we conclude that there must be a $B_{\rm ext}$-dependent sign change of the initialized hole polarization. We have compared Kerr signals for finite and zero magnetic fields for various λ and QWs with widths between 4 and 15 nm and always found a sign-reversal of these hole spins.

We now proceed to analyze the observed dynamics in more detail. The TRKR signal of the localized holes (neglecting the fast-decaying component from the trion spin) is described by

$$\Theta_{\rm K} = A \cdot I_h \left[a_1 e^{-\Delta t/T_1} + a_2 e^{-\Delta t/T_2^*} \cos(\Omega_h \Delta t) \right], \quad (1)$$

where $\Omega_h = g_h \mu_B B_{\rm ext}$. Here, A is the λ-dependent amplitude of the Kerr rotation and $g_h \approx 0.06$ is the hole g factor. The non-oscillating and oscillating parts are proportional to the projection of the respective spin component onto $\mathbf{z}$ and are given by $a_1 = \sin^2\alpha$ and $a_2 = \cos^2\alpha$. They decay with time constants T_1 and T_2^*. The function $I_{\rm h}$ describes the effectiveness of the pump pulse to initialize hole spin polarization. It depends on $B_{\rm ext}$, λ and $P_{\rm P}$. The sign change of the hole spin polarization at low $B_{\rm ext}$ is attributed to a sign change of $I_{\rm h}$.

Figure 1(b) shows the dephasing rates as a function of $B_{\rm ext}$. The decay rates were deduced from fitting Eq. 1 to $\Theta_{\rm K}$ in a time window $100 < \Delta t < 2500$ ps. After a flat region for small $B_{\rm ext}$, $1/T_2^*$ increases about linearly with $B_{\rm ext}$, which is typical for an inhomogeneous broadening of the g factor[11]. A fit of the data in Fig. 1(b) yields a slope of $k_2 = 2.2 \times 10^8$ s^{-1}T^{-1}. Also $1/T_1$ increases with $B_{\rm ext}$ with a slope of $k_1 = 5.7 \times 10^7$ s^{-1}T^{-1}.

To study the initialization at low $B_{\rm ext}$ and the sign reversal, $\Theta_{\rm K}$ was measured at fixed time delay $\Delta t = 12.4$ ns as a function of $B_{\rm ext}$ [see Fig. 2(a)]. The measured curves are well described by Eq. 1, i.e. a $B_{\rm ext}$-dependent cosine function, offset by a non-oscillating part. Note that if T_2^* becomes longer than the laser pulse repetition time of 12.5 ns, the spin polarization created by the previous pump pulses becomes important[12] and the oscillations in $B_{\rm ext}$ deviate from a cosine shape. This is observed in our samples only at $B_{\rm ext} < 0.2$ T, in agreement with the data shown in Fig. 1(b). The sign change of I_h is very well resolved: In Fig. 2(a) we measure dips for $|B_{\rm ext}| < 0.2$ T at every integer spin rotation whereas for $|B_{\rm ext}| > 0.3$ T we measure peaks. Between these two regimes there is a magnetic field $B_{\rm ext,0}$ where $\Theta_{\rm K} = 0$ (marked with a dot and a dashed line). At this field, the initialization of hole polarization is ineffective, i.e. $I_{\rm h} = 0$.

Figure 2(b) shows Kerr rotation data vs. $B_{\rm ext}$ for different $P_{\rm P}$ (left panel) and λ (right panel). The curves are offset for clarity and the dashed line indicates $\Theta_{\rm K} = 0$ for every curve. The black dots mark $B_{\rm ext,0}$. We find a trend towards higher values of $B_{\rm ext,0}$ for increased $P_{\rm P}$ or lower λ. In order to understand and fit the measured curves we now proceed to calculate $I_{\rm h}$.

The dynamics of the initialization process involves the transfer between the four states depicted in Fig. 1(c). Before the arrival of a pump pulse, a localized hole spin has the same probability to be in an up or in a down state $p_{\Delta t=0}(|\Uparrow\rangle) = p_{\Delta t=0}(|\Downarrow\rangle) = 0.5$. Without loss of generality, we assume a σ^- pulse to arrive at Δt=0. Due to optical selection rules, the pulse pumps $|\Uparrow\rangle$-holes into $|\Downarrow\Uparrow\uparrow\rangle$-trions with a probability p_σ. We assume pure heavy-hole states and neglect any interaction of the pump with light holes. This is justified since light holes are sufficiently far away in energy. For $B_{\rm ext}$=0, the trions decay with the carrier decay rate $1/\tau_{\rm R}$ into the original spin state with no resulting polarization. Since $\tau_{\rm R} \ll T_2^*, T_1$, the hole spin decay is neglected for calculating $I_{\rm h}$. For $B_{\rm ext} \neq 0$, the trion spin precesses with a frequency Ω_e, whereas the hole spin precesses with a lower frequency (Ω_h) due to the smaller g factor. The trions therefore do not decay into the original spin state. The result is a positive I_h increasing with $B_{\rm ext}$.[6]

In the experiment, we observe a $|\Uparrow\rangle$ polarization for $B_{\rm ext} = 0$, i.e. a negative I_h. In order to explain this observation, we introduce a process X that pumps $|\Downarrow\rangle$-holes into $|\Downarrow\Uparrow\uparrow\rangle$-trions. We assume this transition to be fast compared to τ_R. A possible mechanism is discussed below. Both processes (σ and X) pump localized holes into the $|\Downarrow\Uparrow\uparrow\rangle$-trion state [see Fig. 1(c)] and the total occupation probability of this state is given by $p_\sigma p_{\Delta t=0}(|\Uparrow\rangle) + p_X p_{\Delta t=0}(|\Downarrow\rangle)$=0.5$[p_\sigma + p_X]$. For $B_{\rm ext} = 0$ and finite p_X, this results in a negative Kerr signal after the decay of the trions.

The system shown in Fig. 1(c) is described by an analytically solvable system of rate equations that include the precession of the spins, the dephasing of the holes and the decay of the trions.[6] Eq. 1 is the solution of this system and

$$I_{\rm h} = \frac{p_\sigma}{2}\left[1 - \frac{p_X}{p_\sigma} - \frac{1+\frac{p_X}{p_\sigma}}{\Omega_{e-h}^2\tau_R^2+1}\right]. \qquad (2)$$

In Eq. 2, $\Omega_{e-h} = |g_e - g_h|\mu_B B_{\rm ext}/\hbar$. We assume p_σ and p_X to be independent of $B_{\rm ext}$. For $B_{\rm ext} = 0$, we recover $I_{\rm h} = -p_X$, i.e. the spin-polarization is only determined by the X process. For finite p_X, I_h has a zero point at finite magnetic field ($B_{\rm ext,0}$). From this point, the ratio of the two pump probabilities can be calculated

$$\frac{p_X}{p_\sigma} = \frac{\Omega_{\rm e\text{-}h,0}^2\tau_{\rm R}^2}{\Omega_{\rm e\text{-}h,0}^2\tau_{\rm R}^2+2}, \qquad (3)$$

with $\Omega_{\rm e\text{-}h,0} = |g_e - g_h|\mu_B B_{\rm ext,0}/\hbar$.

For the next step, we use Eqs. 1-3 to fit the curves in Fig. 2(b). The spin lifetimes are modeled by $1/T_1 = 1/T_{1,0} + k_1 B_{\rm ext}$ and $1/T_2^* = 1/T_{2,0}^* + k_2 B_{\rm ext}$. The measured parameters are $g_{\rm e} = 0.34$, $\tau_{\rm R} = 80$ ps and $B_{\rm ext,0}$ that varies with $P_{\rm P}$ and determines through Eq. 3 the ratio p_σ/p_X. For each value of $P_{\rm P}$, fit parameters k_1, k_2, g_h, c_1 and c_2 are determined, where $c_1 = Ap_\sigma a_1 e^{-\Delta t/T_{1,0}}$ and $c_2 = Ap_\sigma a_2 e^{-\Delta t/T_{2,0}^*}$ are the $B_{\rm ext}$-independent amplitudes of the non-oscillating and oscillating parts of the signal. The assumed linear increase of the spin relaxation rate with $B_{\rm ext}$ overestimates the Kerr signal below 0.2 T. To account for this we weighted the least-square residuals with $B_{\rm ext}^2$ for fitting the curves in the range between 0 and 1 T. The solid black lines in Fig. 2(b) are the resulting fits. The agreement between the data and the fit is very good for $B_{\rm ext} > 0.2$ T.

The fit parameters as a function of $P_{\rm P}$ are displayed in Fig. 3(a). The values for k_1 and k_2 match the results shown as a cross that were obtained from measurements of $\Theta_{\rm K}$ versus Δt [see Fig. 1(a) and (b)]. This demonstrates that the field-dependence of $\Theta_{\rm K}$ measured in Fig. 2 is well described by our model and yields the same $B_{\rm ext}$-dependence for both T_1 and T_2^*. Only small changes on the fit parameters are observed as a function of P_P, reflecting the notion that the pump-power dependence of I_h is the main cause for the difference between the curves in Fig. 2. For increased P_P, g_h decreases by almost 10% which could be attributed to the high sensitivity of g_h on changes in the electrostatic confinement.[7]

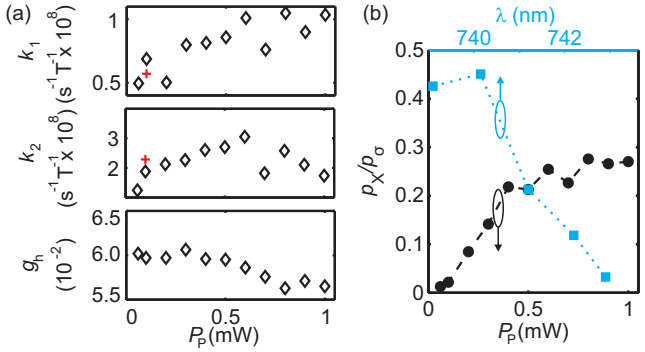

FIG. 3: (Color online) (a) Parameters of the fits vs. pump power $P_{\rm P}$ as described in the text (diamonds) and for comparison fit results obtained from the data shown in Fig. 1(b) (crosses) (b) Ratio of the two pumping mechanisms as a function of $P_{\rm P}$ (dots) and λ (squares).

From the values of $B_{\rm ext,0}$, we derive the ratio p_X/p_σ. The points plotted in Fig. 3(b) are an average of $|B_{\rm ext,0}|$ for the two points obtained by a magnetic field sweep from -1 T to 1 T. The black dots show the ratio as a function of $P_{\rm P}$ for λ = 741.2 nm. The ratio increases and saturates at a value of 0.25 for $P_{\rm P} > 0.5$ mW. By changing the wavelength and keeping the pump power at 0.5 mW, even larger ratios can be obtained. For λ outside the range of the data shown in Fig. 3(b), no hole signal was detected, which we relate to a decrease of the Kerr sensitivity A. The obtained p_X/p_σ-ratios depend on $\tau_{\rm R}$ and would be higher if $\tau_{\rm T}$ were not limited by the recombination.

Finally, we discuss the mechanism X that pumps the $|\Downarrow\rangle$-holes to the $|\Downarrow\Uparrow\uparrow\rangle$-trions. The σ^--pulses also create free $|\Downarrow\uparrow\rangle$-excitons in the QW. The hole spins in the excitons have a much higher relaxation rate than the electron spins[13,14], leading to a conversion of bright excitons into $|\Uparrow\uparrow\rangle$-excitons. These dark excitons can combine with lo-

calized $|\Downarrow\rangle$-holes[15,16] to form a $|\Downarrow\Uparrow\uparrow\rangle$-trion. This process results in a transition X, explaining the negative $I_{\rm h}$ at low $B_{\rm ext}$. Note that the bright excitons can also be captured by a $|\Uparrow\rangle$-hole. In our experiment, this process can not be differentiated from direct excitation of a $|\Downarrow\Uparrow\uparrow\rangle$-trion and is therefore included in p_σ.

With these processes we can qualitatively explain the data in Fig. 3(b). The trion formation with probability p_σ is a process that involves first the generation of an electron-hole pair and then the capturing of a resident hole. Because of the limited availability of resident holes, an increase in $P_{\rm P}$ decreases the average probability p_σ that the created electron-hole pairs can capture $|\Uparrow\rangle$ holes, and increases the probability p_X for a spin flip of the photo-created holes, i.e. the formation of dark excitons, and the subsequent capturing of still available $|\Downarrow\rangle$ hole spins. This explains the increase of p_X/p_σ with pump power. The saturation at $P_{\rm P} = 0.5$ mW is governed by the rates describing the capturing and the spin-flip processes of the excitons. At this pump power, the finite number of localized holes also limits p_X for very large $P_{\rm P}$. A shorter λ increases the p_X/p_σ-ratio for the same reason: The absorption of photons increases for shorter λ, and more electron-hole pairs are generated at same pump power. In addtion, a more pronounced hole dephasing for non-resonantly pumped excitons[13] may favor process X with decreasing λ. The oscillation in the data of $\Theta_{\rm K}$ at zero field in Fig. 2(b) has a smaller amplitude than the fits, showing the limitation of our model that assumes p_X to be independent of $B_{\rm ext}$ and neglects the time-evolution of the excitonic states. The smaller peak is compatible with assuming that the formation of dark excitons is suppressed for small $B_{\rm ext}$. A reason for this could be the spin dynamics of the excitons under the combined influence of both an external and anisotropic exchange splitting[17,18].

To conclude, we find that localized hole spins can be spin-polarized by exploiting the difference in g factor between holes and trions or via the capturing of dark excitons. These two mechanisms lead to the initialization of spin polarization of opposite signs, and their relative strength can be controlled by magnetic field, pump power and wavelength of the pump pulses. By changing these parameters, the size and sign of the spin polarization of localized holes can be controlled.

We thank the SNF and the KTI for financial support. Stimulating discussion with R. Allenspach, A. Fuhrer, T. Korn, M. Kugler, M. Syperek and D. R. Yakovlev are acknowledged.

[1] D. Heiss, S. Schaeck, H. Huebl, M. Bichler, G. Abstreiter, J. J. Finley, D. V. Bulaev, and D. Loss, Phys. Rev. B **76**, 241306 (2007).

[2] D. Brunner, B. D. Gerardot, P. A. Dalgarno, G. Wust, K. Karrai, N. G. Stoltz, P. M. Petroff, and R. J. Warburton, Science **325**, 70 (2009).

[3] A. Zrenner, L. V. Butov, M. Hagn, G. Abstreiter, G. Böhm, and G. Weimann, Phys. Rev. Lett. **72**, 3382 (1994).

[4] H. F. Hess, E. Betzig, T. D. Harris, L. N. Pfeiffer, and K. W. West, Science **264**, 1740 (1994).

[5] M. Syperek, D. R. Yakovlev, A. Greilich, J. Misiewicz, M. Bayer, D. Reuter, and A. D. Wieck, Phys. Rev. Lett. **99**, 187401 (2007).

[6] T. Korn, M. Kugler, M. Griesbeck, R. Schulz, A. Wagner, M. Hirmer, C. Gerl, D. Schuh, W. Wegscheider, and C. Schüller, New J. Phys. **12**, 043003 (2010).

[7] M. Kugler, T. Andlauer, T. Korn, A. Wagner, S. Fehringer, R. Schulz, M. Kubová, C. Gerl, D. Schuh, W. Wegscheider, P. Vogl, and C. Schüller, Physical Review B (Condensed Matter and Materials Physics) **80**, 035325 (2009).

[8] X. Marie, T. Amand, P. Le Jeune, M. Paillard, P. Renucci, L. E. Golub, V. D. Dymnikov, and E. L. Ivchenko, Phys. Rev. B **60**, 5811 (1999).

[9] I. A. Yugova, A. A. Sokolova, D. R. Yakovlev, A. Greilich, D. Reuter, A. D. Wieck, and M. Bayer, Phys. Rev. Lett. **102**, 167402 (2009).

[10] B. D. Gerardot, D. Brunner, P. A. Dalgarno, P. Ohberg, S. Seidl, M. Kroner, K. Karrai, N. G. Stoltz, P. M. Petroff, and R. J. Warburton, Nature **451**, 441 (2008).

[11] S. A. Crooker, J. Brandt, C. Sandfort, A. Greilich, D. R. Yakovlev, D. Reuter, A. D. Wieck, and M. Bayer, Phys. Rev. Lett. **104**, 036601 (2010).

[12] J. M. Kikkawa and D. D. Awschalom, Phys. Rev. Lett. **80**, 4313 (1998).

[13] T. C. Damen, L. Via, J. E. Cunningham, J. Shah, and L. J. Sham, Phys. Rev. Lett. **67**, 3432 (1991).

[14] B. Baylac, X. Marie, T. Amand, M. Brousseau, J. Barrau, and Y. Shekun, Surface Science **326**, 161 (1995).

[15] A. Shabaev, E. A. Stinaff, A. S. Bracker, D. Gammon, A. L. Efros, V. L. Korenev, and I. Merkulov, Phys. Rev. B **79**, 035322 (2009).

[16] B. Eble, C. Testelin, F. Bernardot, M. Chamarro, and G. Karczewski, ArXiv e-prints (2008).

[17] E. Blackwood, M. J. Snelling, R. T. Harley, S. R. Andrews, and C. T. B. Foxon, Phys. Rev. B **50**, 14246 (1994).

[18] D. Gammon, E. S. Snow, B. V. Shanabrook, D. S. Katzer, and D. Park, Phys. Rev. Lett. **76**, 3005 (1996).